Surface phonons and CH vibrational modes of diamond (100) and (111) surfaces

S.-Tong Lee and G. Apai
Corporate Research Laboratories, Eastman Kodak Company, Rochester, New York 14650
(Received 5 October 1992; revised manuscript received 5 April 1993)

The surface phonons and CH vibrational structure of diamond (100) and (111) surfaces have been examined using high-resolution electron-energy-loss spectroscopy. Experimental phonon features of (2×1)-reconstructed diamond surfaces [H-free (100) and partially H-terminated (111)] agree well with scaled phonon frequencies of theoretically predicted modes for similarly reconstructed silicon surfaces. Several modes not detected on silicon surfaces are observed on diamond surfaces, in agreement with scaled theoretical calculations. Vibrational spectra from hydrogen-terminated diamond (1×1) surfaces reveal several types of CH_x species, including sp^3 hybridized methyl and methylene groups, and olefinic (sp^2 hybridized) methylene groups. On heating to $\sim$1473 K, hydrogen desorbs readily from the (100) surface. Complete removal of hydrogen from the (111) surface by repeated annealing to $\sim$1473 K was impossible, although (2×1) reconstruction had already occurred.

I. INTRODUCTION

Until a few years ago, interest in diamond single-crystal surfaces was predicated on their structural similarity to silicon. Most of the earlier studies of these diamond surfaces[1] were thus aimed at gathering more information about silicon surfaces. With the recent demonstration that diamond thin films can be synthesized at a high rate,[2] allowing significant technological potential, surface-science interest is now redirected to the diamond surface itself.

Previous studies have shown that surfaces of diamond are normally terminated by hydrogen,[1,3–8] which stabilizes the simple truncated-bulk surface structure of (1×1) symmetry via interaction with the dangling bonds of the surface carbon atoms. Hydrogen begins desorbing from the surfaces at $\geq$1273 K, and the resulting surfaces reconstruct to achieve a (2×1) symmetry.[1,3–8] Using high-resolution electron-energy-loss spectroscopy (HREELS), Waclawski *et al.*[6] measured the vibrational spectrum of the diamond (111) surface, and provided direct evidence that this surface is terminated by hydrogen. Hamza and co-workers[7,8] used time-of-flight mass spectrometry to study the hydrogen desorption process from diamond (100) and (111) surfaces and the accompanying surface reconstruction. In spite of these studies, a clear picture of the types of CH_x species existing on hydrogen-terminated diamond surfaces is not presently available. To our knowledge, surface phonons of diamond have not been observed previously. In light of the great interest concerning silicon surface reconstructions and the usefulness of HREELS to probe optically active surface phonons, diamond studies merit attention. Diamond surface phonon studies should provide additional interesting data for understanding semiconductor surfaces and for comparison with future theoretical calculations of phonons on diamond surfaces.

Diamond films can be routinely grown at a high rate by low-pressure chemical vapor deposition (CVD), using a gas mixture of hydrocarbon (typically methane) highly diluted with hydrogen.[2] The hydrogen-terminated diamond surface plays a major role in diamond growth by CVD. In the presence of atomic hydrogen, diamond growth rather than graphite deposition becomes the primary process. Aside from its ability to preferentially etch graphite, hydrogen atoms are also known to stabilize the diamond surface by tying up the dangling bonds of carbon, as well as promoting sp^3 hybridization of carbon.[2] Ironically, as much as it is needed, hydrogen eventually has to desorb from the surface to allow for continued diamond growth by CVD. Questions such as why diamond grows best on (100) diamond surfaces, how the structure of H-terminated diamond surfaces affects diamond growth, how hydrogen desorbs from and bonds to diamond surfaces, are all important for understanding diamond growth processes. An understanding of the diamond surface structure and chemisorption processes occurring at the surfaces may provide insight into these questions. This paper addresses a number of these questions. We provide evidence for surface phonon modes intrinsic to the diamond (100) and (111) crystals and the presence of aliphatic and olefinic CH_x species on the respective hydrogen-terminated surfaces.

II. EXPERIMENT

Three $4\times4\times0.25$ mm diamond crystals polished, cleaned, and supplied by Drukker International were used in this study. These crystals are, respectively, type-IIa (100), -IIb (100) (boron doped and semiconducting), and -IIa (111) diamond. Before loading into vacuum, each crystal was boiled for a few minutes in a 1:1:1 solution of HNO_3-$HClO_4$-H_2SO_4, rinsed in distilled water, washed in acetone, then ethanol, and finally blown dry with nitrogen. Samples were loaded into ultrahigh vacuum (UHV) through a sample transfer chamber, previously described.[9] The high-resolution electron-energy-loss and low-energy-electron-diffraction (LEED) measurements were performed using a Vacuum Generators ESCALAB system with a base pressure of mid 10^{-11}

0163-1829/93/48(4)/2684(10)/$06.00

Torr. All measurements were performed with the sample at room temperature. The energy resolution, as measured by the full width at half maximum (FWHM) of the elastic peak, was approximately 10 meV, and the loss spectra were recorded in the specular mode with a scattering angle of 90°. Electron energies were typically 5 eV. Vacuum heating was done by wrapping the diamond crystal in a tantalum foil heater. Temperature measurement was obtained by a combination of an optical pyrometer and an *N*-type thermocouple, spot welded behind the Ta foil. Hydrogen atom dosing was accomplished by placing the diamond crystal 2 cm in front of a tungsten filament heated in a 10^{-6}-Torr hydrogen ambient.

Deconvolution techniques in HREELS have become important and successful toward understanding chemisorption phenomena on oxide surfaces,[10,11] correlating surface phonon spectra with dielectric theory calculations,[9] and analyzing polymer surface scattering.[12,13] We use a deconvolution resolution enhancement method, based upon the nonlinear predictor method of maximum likelihood,[14] to generate from the electron-energy-loss spectrum a schematic display of spectral components which provides a concise means of discussing the CH vibrational data. The referenced applications have shown that accurate additional information about HREEL data can be obtained, because the instrumental convolution function provided by the elastic peak is always available for each reflection energy-loss spectrum.

III. RESULTS

A. Low-energy electron diffraction and Auger characterization

Most of the diamond surfaces exhibited a faint (1×1) LEED pattern after loading in vacuum. Nonetheless, a well-defined (1×1) LEED pattern was always obtained after the diamond surface was heated to 1023 K. Upon heating the surfaces to ~1473 K, the (1×1) LEED patterns of (100) and (111) diamond surfaces both changed to an apparent (2×2) symmetry. This observation is in agreement with previous reports[1,3,6–8] that both (100) and (111) surfaces exhibit a (2×1) reconstruction upon hydrogen desorption. The observed (2×2) LEED pattern of the (100) surface is a superposition of two rotated domains of (2×1) symmetry, while the observed (2×2) pattern of the (111) surface results from three rotated domains of (2×1) symmetry.[1] These annealed, reconstructed (2×2)-(2×1) surfaces can be reversibly converted to (1×1) symmetry by atomic hydrogen dosing.

Diamond surfaces were also examined using Auger electron spectroscopy. Our carbon (*KVV*) Auger line shapes for hydrogen-free (100)-(2×1) and partially H-terminated (111)-(2×1) diamond surfaces are similar to those attributable to clean diamond surfaces by Pate[1] and Lurie and Wilson.[3] Further evidences from HREELS phonon structure and correlations with scaled theoretical calculations for reconstructed silicon surfaces will argue against graphite-related modes.

B. Electron-energy losses due to diamond surface phonons

Vibrational electron-energy-loss spectra could be readily measured from all the diamond samples used in this study, and energy resolution did not appear to be significantly affected by the insulating properties of diamond. Typical energy-loss spectra of diamond surfaces, obtained after several heating cycles to 1473 K in UHV, are shown in Figs. 1(a) and 1(b) for (100)-(2×1) and (111)-(2×1) surfaces, respectively. These spectra were recorded when they showed no changes upon further high-temperature heating cycles. Those vibrational features that persist and do not diminish with continued heating cycles (i.e., decreasing surface hydrogen) were attributed to intrinsic diamond behavior. In the case of the (100) surface, all hydrogen was desorbed and identical spectra were observed for both type-IIa and -IIb diamonds, indicating that the boron dopant caused no changes in the energy-loss spectrum. Although a small amount of residual hydrogen could not be eliminated from the (111) surface upon annealing to ~1473 K, the development of the intrinsic vibrational structure was similar to that of the (100) surface. Although we cannot be certain that subtraction of residual CH features will produce only the intrinsic structure, we do it to more clearly show the diamond (111) intrinsic loss features in Fig. 1(c). We interpret the electron-energy-loss features from the annealed, reconstructed diamond surfaces to be associated with intrinsic surface phonon excitations. The (100)-(2×1) surface exhibits three phonon bands at 87 (700 cm^{-1}), 126 (1015 cm^{-1}), and 152 (1225 cm^{-1}) meV. The (111)-(2×1) surface shows clearly two phonon bands

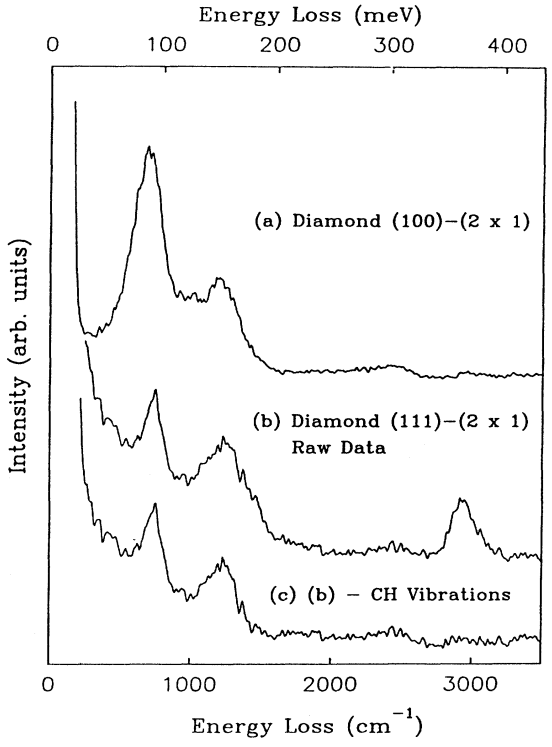

FIG. 1. Vibrational energy-loss spectra of (a) (100)-(2×1) and (b) (111)-(2×1) diamond surfaces, which were obtained after several cycles of annealing to 1473 K. (c) Spectrum *b* with CH vibrational structure removed.

at 92 (740 cm^{-1}) and 153 (1235 cm^{-1}) meV and possibly a third band at ~120 meV (970 cm^{-1}). The positive identification of the 120-meV band is precluded by the interference from the remnant CH vibrations. The feature near 300 meV for both surfaces is attributable to a multiple loss of the ~150-meV band.

The 153-meV (1235-cm^{-1}) phonon feature of the (111) surface is complicated by the CH vibrational excitations arising from hydrogen remaining on the surface. It was not possible to completely remove hydrogen from the (111) surface even after repeated heating to ~1473 K, as indicated by the persistent presence of a weak CH stretching vibration near 363 meV (2930 cm^{-1}). Hydrogen presence is clearly evident in Fig. 1(b), which represents the least amount of hydrogen that remains on the (111) surface after repeated heating cycles. Because of the remaining hydrogen, the 153-meV phonon loss peak of the (111) surface derives some intensity, particularly on the higher-energy-loss side, from CH deformation modes. In contrast to the (111) surface, the (100) diamond surface is more easily cleaned of hydrogen, as readily manifested by the lack of any CH stretch vibrations near 360 meV [Fig. 1(a)]. We note further that for both surfaces the intensity of the lowest-energy phonon feature increases relative to that of the high-energy phonon feature with a decreasing amount of hydrogen on the surface. Our loss spectra show no large inelastic continuum with a Drude-type tail, as described previously.[6]

C. Vibrational energy losses on hydrogen-terminated diamond surfaces

The gross features of the energy-loss spectra obtained from all as-loaded diamond surfaces were generally similar, albeit there were slight differences among spectra in the intensity profiles of the energy-loss bands [see Figs. 2(a) and 2(b)]. Such differences are attributable to slight variations in surface hydrogen and hydrocarbon concentrations and are understandable in view of the uncontrolled conditions under which the diamond surfaces were exposed before UHV cleaning. In spite of the slight variations, several features common to all spectra are worth noting. Analysis of energy losses from all diamond surfaces following etching, rinsing, and introduction into the spectrometer chamber always showed a broadband between 80 (650 cm^{-1}) and 210 (1690 cm^{-1}) meV, and an intense peak near 363 meV (2930 cm^{-1}), most likely indicative of both hydrogen termination and hydrocarbon adsorption. Photoemission, Auger, and HREEL spectroscopies showed that no inorganic impurities were detected on the as-loaded diamond surfaces. For the as-loaded diamond (100) surface annealed to 423 K, we thus attribute the energy-loss signals to the vibrational excitations of the surface species resulting from hydrogen termination and weakly adsorbed hydrocarbon species on the diamond surfaces. When the as-loaded diamond was heated to 923 K, both the high and low vibrational bands narrowed and became more defined, as exemplified in Fig. 2(c). The resulting spectrum became more similar to that obtained from a hydrogen-terminated diamond surface [Fig. 3(a)] prepared by thermal dehydrogenation, followed by dosing with atomic hydrogen. This similarity can be interpreted to mean that the adsorbed hydrocarbons and water are readily desorbed by 923 K,[15] and the moderately annealed diamond surface more closely resembles a purely hydrogen-terminated surface.

The UHV-formed hydrogen-terminated diamond surfaces were prepared by first desorbing hydrogen from the as-loaded diamond surfaces by annealing to ~1473 K, whereupon the surface reconstructed to (2×2)-(2×1) symmetry. The amount of surface hydrogen was monitored by the intensity of the CH stretch bands near 363 meV (2930 cm^{-1}). Once the intensity of this band reached a negligible [e.g., on the (100) surface] or steady-state level [e.g., on the (111) surface], the diamond surface was then dosed with atomic hydrogen. Hydrogen dosing converted the LEED pattern to (1×1) from the reconstructed (2×2)-(2×1) pattern. The energy-loss spectra obtained from these hydrogen-terminated diamond surfaces are displayed in Fig. 3. Histograms of deconvoluted dominant bands are shown for each spectrum to provide a concise means for the discussion of results. The spectra of the diamond (100)-(1×1)-H and (111)-(1×1)-H surfaces show multiple vibrational modes between 93 (750 cm^{-1}) and 181 (1460 cm^{-1}) meV, and overlapping CH stretch modes in the region near 363 meV (2850–3070 cm^{-1}).

The hydrogen-terminated vibrational spectra for both

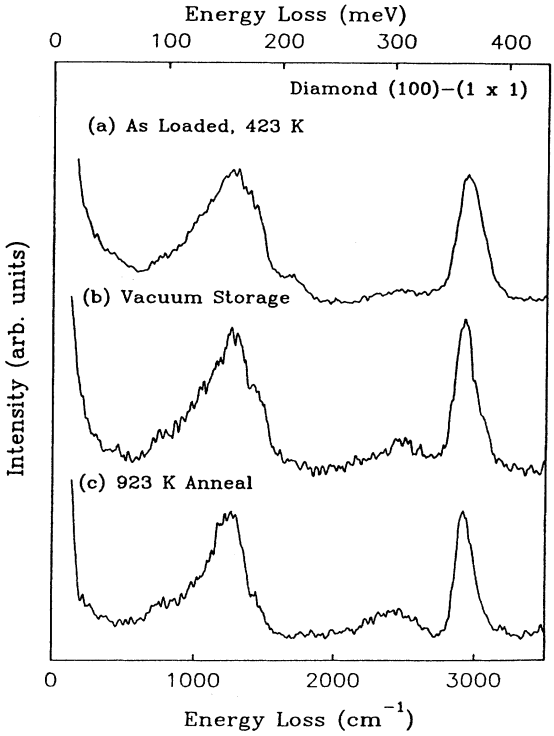

FIG. 2. Vibrational energy-loss spectra of the (a) as-polished and etched diamond (100)-(1×1) surface after heating to 423 K in UHV, (b) diamond (100)-(1×1) surface after heating to 1473 K in UHV and storing in an unpumped high vacuum for several days, and (c) diamond surface in (a) after heating to 923 K.

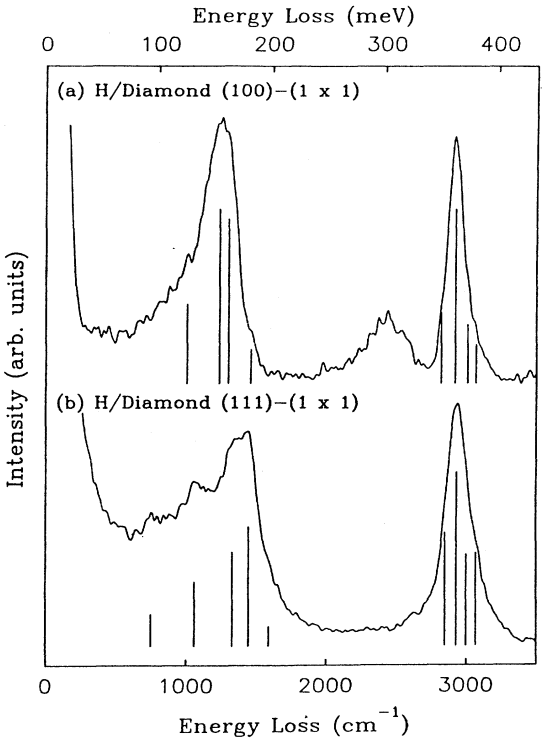

FIG. 3. Vibrational energy-loss spectra of the (a) (100)-(1×1) H-terminated and (b) (111)-(1×1) H-terminated diamond surfaces after heating to 1473 K and subsequent atomic hydrogen dosing. Histograms represent CH vibrational modes assigned from the deconvolution of the spectra.

diamond surfaces provide sufficient detail to make several meaningful comparisons as to the observed differences in the spectral components as a function of surface orientation, with or without deconvolution methods. Here, we use the results of spectral deconvolution to discuss the results more concisely. The efficacy of this type of analysis has been documented.[9–14] In the CH_x stretching region, the broadness and asymmetry of the features indicate a distribution of modes attributable to various CH_x-type species, aliphatic (sp^3 hybridized) and olefinic (sp^2 hybridized). Hydrogen-terminated diamond (100) surfaces show CH_x stretching modes near 350 (2820 cm^{-1}), ~361 (2915 cm^{-1}) broadband, 374 (3010 cm^{-1}), and 381 (3070 cm^{-1}) meV. For hydrogen-terminated diamond (111) surfaces we observe CH_x stretch modes near 353 (2850 cm^{-1}), ~363 (2930 cm^{-1}) broadband, 372 (3000 cm^{-1}), and 381 (3070 cm^{-1}) meV. Without deconvolution, it is apparent that the CH stretch region for the hydrogen-terminated diamond (100) surface is substantially narrower than it is for the hydrogen-terminated (111) surface in agreement with the histograms. It is apparent that the additional broadness on H-diamond (111) extends above 3000 cm^{-1}, indicative of olefinic CH stretch modes. We also observe significant intensity in the CH_x deformation and wag regions of the loss spectra, indicating that multiple hydrogens (e.g., —CH_2,—CH_3) terminate the diamond surface. Again the majority of relevant bands can be discerned visually, and taking into account the energy-loss backgrounds in Fig. 3, an estimate of relative intensities can be made. We use spectral deconvolution as an aid to eliminate bias. CH_x deformation modes for the H-diamond (100) surface are observed near 125, (1005 cm^{-1}), 153 (1235 cm^{-1}), 162 (1300 cm^{-1}), and 181 (1460 cm^{-1}) meV. On the H-diamond (111) surface these CH_x deformation modes occur near 93 (750 cm^{-1}), 132 (1060 cm^{-1}), 165 (1330 cm^{-1}), 179 (1445 cm^{-1}), and 198 (1600 cm^{-1}) meV. While the majority of the observed modes for both surfaces are quite similar in frequency, there exist major differences in the intensities of several modes. The intense ~1450-cm^{-1} mode on the H-diamond (111) surface is accompanied by low-intensity features near 1600 and 750 cm^{-1}. On the H-diamond (100) surface, the 1450-cm^{-1} mode is weak with no accompanying peak near 1600 cm^{-1} and very little intensity near 750 cm^{-1}. The broad mode near 1235 cm^{-1} on the H-diamond (100) surface is not resolved on the H-diamond (111) surface. These differences in hydrogen-associated vibrational bands suggest that the concentrations of different termination groups vary between the two surface orientations.

Table I provides a summary of the estimated CH vibrational mode frequencies and their assignments, based on frequencies determined by spectral deconvolution. A qualitative measure of the deconvoluted band intensities

TABLE I. Frequencies in meV (cm^{-1}) of energy-loss peaks due to CH vibrations on diamond (100) and (111) surfaces obtained by spectral deconvolution and shown as histograms in Fig. 3.

(100)	(111)	Assignment
381 (3070)	381 (3070)	asymmetric olefinic CH stretch
374 (3010)	372 (3000)	symmetric olefinic CH stretch
~361 (2915)	~363 (2930)	asymmetric aliphatic CH stretch
350 (2820)	353 (2850)	symmetric aliphatic CH stretch
	198 (1600)	C=C stretch
181 (1460)	179 (1445)	aliphatic and olefinic CH deformation
162 (1300)	165 (1330)	—CH_3 deformation
153 (1235)		tertiary bonded CH rock
125 (1005)	132 (1060)	mixed mode CH rock and C—C stretch
	93 (750)	olefinic =CH_2 wag and aliphatic —CH_2 rock

is provided by the histogram intensities in Fig. 3. The assignment of nearly identical vibrational frequencies for both surfaces and their correlations with expected group frequencies (cf. Sec. IV B) provide confidence in the deconvolution procedure. The loss feature near 305 meV (2460 cm^{-1}) appearing most strongly on the H-terminated (100) surface is attributable to a multiple loss of the strong 150–155-meV (1210–1250-cm^{-1}) CH deformation mode region. We do not have an explanation for the weakness of this multiple loss feature on the H-diamond (111) surface.

IV. DISCUSSIONS

Electron-energy-loss spectra have been measured on clean diamond (111)-(2×1) surfaces by Waclawski *et al.*[6] They were unable to observe phonon excitations, although they did observe a small feature near 170 meV (1370 cm^{-1}), which they suggested to be a carbon-carbon loss. Waclawski *et al.*[6] instead observed an inelastic continuum with a Drude-type tail to the loss side of the elastic peak, which they attributed as resulting from a two-dimensional metallic behavior of the dangling-bond surface states on the diamond (111)-(2×1) surface. We believe that insufficient energy resolution and a high inelastic background near the elastic peak made it difficult for Waclawski *et al.* to detect the phonon modes. In the present study, for both reconstructed diamond (100) and (111) surfaces, the intrinsic phonon modes on diamond surfaces were quite easily observed. We do not find a large broadening of the elastic peak or the severe Drude-type tail upon desorption of hydrogen from the hydrogen-terminated surfaces. We attribute our success in recording the surface phonons to the higher-energy resolution, i.e., <10 meV, that was achievable in our measurements. Aside from the instrumental resolution, the achievable resolution on a highly insulating type-IIA diamond (its bulk resistivity is as high as 10^{13} Ω cm), without the need of charge neutralization, is further allowed by a high surface conductivity. The conductivity derives from a high density of surface defects, which inevitably exist on a polished diamond surface.

A. Diamond surface phonons

Both diamond and silicon are characterized by fourfold-coordinated sp^3 bonding of O_h symmetry. Based upon the symmetry of the bulk crystal structure, these materials have no polarization, and hence no dipole field associated with long-wavelength phonons. However, at the surface this restriction is relaxed. Thus, Ibach[16] detected a phonon excitation at ~56 meV on the silicon (111)-(2×1) surface, and attributed this excitation to strong interaction of low-energy electrons with surface phonons. More recent experimental observations place the mode closer to 58 meV.[17] Initially, justification for strong dipole interactions was that the two atoms in the unit cell of silicon are in different positions with respect to the surface, creating an effective ionic charge. More recent theoretical studies of the surface phonon modes in silicon have indicated that surface reconstruction is responsible for the strong dipolar character of the observed surface phonon mode. Because clean diamond surfaces exhibit similar reconstruction (2×1) to those known for clean Si surfaces, it may thus be expected that the surface phonon modes of diamond and silicon should be correlated. The diamond phonon modes may be estimated by an appropriate scaling of those for silicon. Such a procedure has been used by Shroder, Nemanich, and Glass[18] in scaling the bulk density of states of amorphous silicon to model that of amorphous diamondlike materials. In view of the lack of experimental and theoretical work on the surface phonons of diamond, we will draw heavily from information about silicon surfaces in discussing and understanding the present results.

Let us first discuss the phonon modes for the diamond (111)-(2×1) surface that correlate with experimentally determined surface phonons for Si. Experimentally, a single strong dipole-active phonon band near 58 meV has been observed by HREELS on the clean Si (111)-(2×1) surface.[16,17] Using this silicon phonon energy and the scaling factor (2.56) derived from the ratio of first-order Raman modes of the crystalline form of silicon and diamond [Si=64.5 meV (520 cm^{-1}); diamond=165.1 meV (1333 cm^{-1})], we obtain the corresponding surface phonon of diamond at 149 meV. This value agrees remarkably well with our observed diamond phonon band at 153 meV. The agreement lends support to our interpretation that the observed energy-loss feature is associated with surface phonon excitations. An acoustic-phonon excitation on the silicon (111)-(2×1) surface has been measured at 10 meV by He-atom inelastic scattering.[19] HREELS has not detected this low-energy mode, presumably due to the interference from the strong diffuse elastic intensity. The corresponding phonon excitation on the diamond (111)-(2×1) surface estimated from scaling is at 25.6 meV, which is not evident in our spectrum, most likely also due to interference from the tailing of the elastic peak.

The structure of the silicon (111) surface has been extensively studied. Both experimental[17,20–28] and theoretical[29,30] studies have provided expanding evidence favoring the π-bonded chain model proposed by Pandey[29] as the structure of the reconstructed silicon (111)-(2×1) surface. This model involves the formation of π-bonded chains of silicon atoms oriented along one of three equivalent [110] directions of the surface plane. For the reconstructed diamond (111)-(2×1) surface the π-bonded chain model is also the preferred structure deduced from the ion scattering[31] and two-photon photoelectron spectroscopy[32] studies. A number of theoretical studies[33–38] are available on the phonons of the silicon (111)-(2×1) surface based on the π-bonded chain model. Further support for assignment of surface phonon modes on the diamond (111)-(2×1) surface can be made based upon these silicon (111)-(2×1) phonon calculations. To compare the calculations with the HREEL results on diamond, we again scale the silicon results. The scaled phonon data of silicon (111)-(2×1) calculated by Alerhand and co-workers[33,34] and Miglio *et al.*[35] are displayed in Figs. 4(b) and 4(c), respectively. For ease of comparison, we use the scaled surface phonon density of states for the silicon (111)-(2×1) surface obtained by Alerhand, Allan

and Mele.[33] Both of the theoretical phonon spectra were obtained from the discrete vibrational features by convolution with a Lorentzian with a FWHM of 5 meV, which, after scaling, is comparable to the 8–12-meV energy resolution used to record our loss spectra. These calculations were done using the tight-binding theory and bond-charge model by Alerhand and co-workers[33,34] and Miglio and co-workers,[35,36] respectively. Despite the different calculational schemes, the results from both calculations are quite similar. They show that the π-bonded chain model of the silicon (111)-(2×1) surface is capable of providing a very straightforward explanation for the observation of the strong dipole-active phonon at 58 meV by HREELS (Refs. 16 and 17) and the dispersionless phonon band at 10 meV by He ion scattering.[19] In addition, both calculations show that the phonon density exhibits three major regions at 5–23, 23–39, and 45–70 meV (i.e., after scaling, they become 13–60, 60–100, and 115–180 meV in Fig. 4), respectively. The experimental phonon bands at 10 and 58 meV on a silicon (111)-(2×1) surface are thus satisfactorily reproduced as the strongest phonon peaks that fall, respectively, in the lowest- and highest-energy region in the calculated phonon density of states. However, the calculated phonons at 23–39 meV have not been detected or resolved in HREEL spectra due probably to the large diffuse elastic intensity, as suggested by Miglio *et al.*[35] In the case of diamond, the phonon bands are expected to be more accessible to HREEL detection, because carbon is less massive than silicon, and hence the corresponding phonon modes in diamond are shifted to higher energy. This is, in fact, borne out in the experiment [Fig. 4(a)], which shows that two distinct phonon bands are observed at 92 and 153 meV. These two bands are reproduced in the theoretical scaled silicon phonon spectrum and estimated to fall in the energy regions of 60–100 and 115–180 meV, respectively. The asymmetry and width of the 153-meV experimental phonon band suggest more than one phonon mode is involved with this band, which is consistent with the multiple phonon features predicted in this energy region by the calculations. Compared to the scaled spectrum, it is logical to interpret the 153-meV band of diamond to be the equivalent of the intense dipole-active band of silicon at 58 meV. An important phonon mode pointed out by Alerhand, Allan, and Mele[33] is a rocking mode at 34 meV on the Si (111)-(2×1) surface. This scales to 87 meV (700 cm^{-1}) for diamond. Our 92-meV (740-cm^{-1}) feature appears to be this mode.

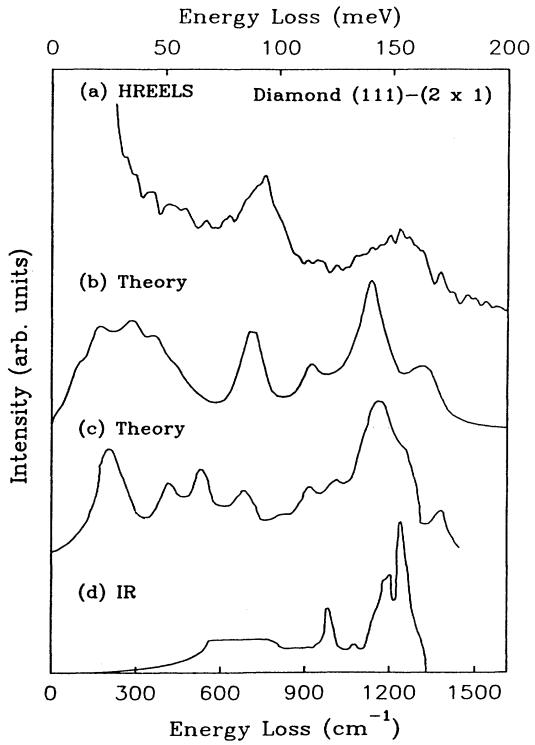

FIG. 4. (a) Vibrational energy-loss spectra of the (111)-(2×1) diamond surface with CH vibrational structure removed [same as Fig. 1(c)]. Scaled silicon (111)-(2×1) theoretical surface phonon data from Ref. 30 (b) and Ref. 32 (c). (d) Experimentally derived infrared one-phonon density of states for bulk diamond from Ref. 46.

Let us now turn to the phonon spectrum of the diamond (100)-(2×1) surface, which is displayed in Fig. 1(a). It consists of two major features at 87 meV (700 cm^{-1}) and 152 meV (1225 cm^{-1}), and a weak feature at 126 meV (1015 cm^{-1}) that can be successfully resolved using deconvolution techniques, as previously discussed. Again, we refer to the existing knowledge of phonons on the silicon (100)-(2×1) surface. Unlike the extensively studied silicon (111)-(2×1) surface, no phonons have been observed on the silicon (100)-(2×1) surface. Although an energy-loss band at 111 meV has been detected on the reconstructed silicon (100)-(2×1) surface,[39,40] the nature of this excitation is not certain, but has been attributed to intrinsic surface defects. In contrast to the lack of phonon modes detected on the silicon (100)-(2×1) surface, the richness of the surface phonon spectrum of the corresponding diamond surface as revealed by HREELS is unexpected.

The ideal silicon (100) surface is terminated by silicon atoms with two dangling bonds. Reducing these unsaturated dangling bonds provides the driving force for the reconstruction at the surface. The standard model of the reconstructed silicon (100) surface involves the formation of tilted surface dimers.[41] Using this model and tight-binding theory, Mele and co-workers[42–44] and Mazur and Pollmann[45] have calculated the surface vibrational excitations for Si (100)-(2×1). The calculations[43] showed that three surface phonons at 25, 44, and 61 meV at the K point of the surface Brillouin zone are of particular interest, as they were predicted to be infrared active and should be accessible to HREEL detection. The first or lowest-energy vibrational mode involves a nearly pure rocking of the surface dimer. The second or medium-energy mode involves a swinging of alternate surface dimers 180° out of phase. The third or highest-energy mode has the largest amplitude on a fully coordinated subsurface atom at which the bond angles are distorted, and the weakest amplitude on the top surface layer. These energies when scaled become 67 (540 cm^{-1}), 113

(910 cm^{-1}), and 156 (1260 cm^{-1}) meV for the corresponding phonon modes in diamond. Our observed energy-loss bands at 126 and 152 meV may be associated with the calculated scaled phonon modes at 113 and 156 meV, respectively, while the calculated scaled phonon mode at 67 meV may be associated with the energy-loss feature observed at 87 meV [Fig. 1(a)].

The above discussion shows that the diamond phonons estimated from a simple scaling of the corresponding calculated phonons on silicon surfaces are in reasonable agreement with the HREEL spectra for both diamond (111)-(2×1) and (100)-(2×1) surfaces. The agreement may be surprising, particularly in view of the less satisfactory agreement in the case of silicon, where, out of the four phonon excitations predicted possible, only two were observed on the silicon (111)-(2×1) surface by HREEL and He ion-scattering experiments, and none on the silicon (100)-(2×1) surface. The contrasting behavior in the vibrational excitations on the diamond and silicon surfaces suggests differences in the lattice dynamics brought about by the less massive diamond lattice as well as the possibility of additional surface defect features. Although the (2×1) reconstructions of diamond are similar to those of silicon, they are not identical. For example, the degree of dimerization of the silicon (111) π-bonded chains and the extent of relaxation are different. We expect no major changes to our scaling treatment; however, some modifications of the normal modes may result. As a result, comparison with future theoretical calculations of diamond surface phonons should provide interesting opportunities for further investigations.

We wish to point out, in addition, that similarities exist among the peak positions in the HREEL spectrum of the diamond (111)-(2×1) surface, the scaled theoretical phonon modes, and the bulk one-phonon density of states of diamond [Fig. 4(d)] derived from the infrared absorption.[46] The agreement of the HREEL spectra for silicon and diamond with theoretical silicon surface phonon modes, unscaled and scaled, respectively, is expected based on selection rules for HREEL measurements. Some similarity of the HREELS diamond data and scaled theoretical phonon modes with a bulk derived phonon density of states may indicate that the defective nature of the diamond surface is a contributing factor.

B. Hydrogen-terminated diamond surfaces

Waclawski *et al.*[6] measured the energy-loss spectrum for the as-polished diamond (111)-(1×1) surface, as well as for hydrogen adsorption on the clean diamond (111)-(2×1) surface. By observing the isotope vibrational shifts for the deuterium-terminated diamond surface, they concluded that the observed energy-loss features were due to CH vibrational excitations. A correspondence of the loss spectrum with the infrared spectrum of ethane led them to conclude that the hydrogen-covered diamond (111) surface contained an appreciable number of carbon atoms in the form of sp^3 hybridized methyl ($—CH_3$) species rather than the singly bonded sp^3 (—CH) species. The latter moiety would have been the logical candidate to be formed on an ideal, unreconstructed diamond (111)-(1×1) surface, since this surface is terminated with each surface carbon atom having a single, sp^3 hybridized dangling bond normal to the surface. Waclawski *et al.*[6] gave three possible mechanisms for the existence of methyl-group terminations, i.e., the presence of surface defects, the corrosive action of hydrogen, and the breakup of the π-bonded chains by hydrogen absorption, so that the surface carbon atoms could end up having three dangling bonds to form the $—CH_3$ species. Their constraints on energy resolution precluded any assignment of other hybridized CH vibrational modes.

Our loss spectrum of the diamond (111)-(1×1)-H surface is in general agreement with that reported by Waclawski *et al.*,[6] although our spectrum is better resolved. For the two H-terminated diamond surfaces studied, we observe multiple hydrogen-terminated carbon atoms as exhibited by CH_x deformation modes. However, it should be pointed out that the energy-loss spectrum is also consistent with the simultaneous presence of various $—CH_{x=1-3}$-type species. In interpreting the loss spectra we refer to the accepted CH vibrational frequencies discussed in standard references.[47–49] First, in the CH stretch region (Fig. 3) the presence of a broadband near 2920 cm^{-1} and a discrete shoulder near 2830–2840 cm^{-1} indicate a distribution of sp^3-type $—CH_2$ and $—CH_3$ species for both surfaces. Nevertheless, the contribution from the sp^3-type —CH species cannot be ruled out. Vibrational modes above 3000 cm^{-1} for both (100) and (111) surfaces are clear indications of olefinic ($=CH_2$) CH stretch modes, which are higher in frequency than the CH stretching vibrations of the aliphatic $—CH_{x=1-3}$ groups. The H-diamond (111) surface shows a slightly higher relative olefinic intensity versus the aliphatic intensity compared with the H-diamond (100) surface; however, this could be coverage dependent. The CH deformation region contrasts most clearly the differences between the two diamond surfaces. On the H-diamond (111) surface there is a weak feature near 1600 cm^{-1} that can be attributed to a delocalized C=C double bond. This feature is not apparent on the H-diamond (100) surface. Along with the C=C feature is an intense 1450-cm^{-1} mode, a 1330-cm^{-1} mode, and a 750-cm^{-1} mode. The 1450- and 1330-cm^{-1} bands are assignable as $—CH_3$ deformation modes. However, the 1450-cm^{-1} mode is also assignable to a $—CH_2$ deformation. Some part of the low-energy side of the 1450-cm^{-1} mode may be due to an olefinic $=CH_2$ deformation, as is the 750-cm^{-1} olefinic $=CH_2$ wag. On the H-diamond (100) surface the 1460-cm^{-1} mode is weak, and a broadband occurs at ~1235 cm^{-1} that cannot be ascertained to be present on the H-diamond (111) surface. The ~1235-cm^{-1} mode on the H-diamond (100) surface is characteristic of tertiary-related CH rock vibrations that mix with C—C stretch vibrations to produce bands near 1245, 1200, and 930 cm^{-1}.[48] The ~1300-cm^{-1} band on this surface may again be assigned to a $—CH_3$ deformation, as is part of the 1460-cm^{-1} mode. The 1005-cm^{-1} mode on the (100) surface and the 1060-cm^{-1} mode on the (111) surface are assignable to mixed-mode CH rock and C—C stretch vibrations. The drastic difference in intensities for the deformation modes on the two diamond

surfaces could be related to orientational ordering and to possible orientation variations of terminal groups. We thus interpret the major intensity differences as being most probably dependent upon the bonding characteristics of the surface carbon network and its orientations. On the other hand, the similarity of both surfaces to terminate in multiple CH_x species (cf. Table I) suggests that the nature of the bonding sites are not so different on the two surfaces. This is understandable because, by virtue of diamond polishing, the finished surfaces are highly defective, thus diminishing the ideal surface behavior. In this respect, diamond surfaces are in contrast to silicon or other crystals whose ideal surfaces can be prepared more easily by conventional methods for surface-science studies.

Reducing the number of unfavorable dangling bonds provides the driving force for both clean (111) and (100) diamond surfaces to reconstruct through pairing of the dangling bonds of neighboring surface carbon atoms. As a result, the diamond (111) surface adopts the π-bonded chain configuration[29] and the (100) surface is terminated with C—C dimers.[41] Adsorption of hydrogen on the reconstructed diamond surfaces, therefore, does not take place with free dangling bonds, but rather involves the breaking of carbon-carbon bonds with the subsequent formation of C—H bonds. The rate-limiting step in the formation of CH bonds is the replacement of an initial C—C bond with a C—H bond. This is energetically favorable, since the C—H bond energy (98.8 kcal/mol) is larger than the C—C bond energy (83.1 kcal/mol).[50] From energy considerations alone, the conversion of C—C bonds to C—H bonds should continue progressively, leading to the sequential formation of —CH, $—CH_2$, $—CH_3$, and eventually to CH_4, which leaves the surface. The reaction of hydrogen to breakup C—C bonds may be mediated by several factors. Steric hindrance may act to slow down or check the reaction of hydrogen with the C—C bonds backbonded to the carbon subsurface layer. On the other hand, surface defects such as vacancies, which are inevitably present on diamond surfaces, may facilitate C—H formation by providing more accessibility. It is worthwhile noting that existing silicon studies[51,52] have already provided clear evidence for the coexistence of —SiH, $—SiH_2$, and $—SiH_3$ species on the silicon (111)-(2×1) surfaces, showing that aggressive behavior of hydrogen does occur on silicon,[51] an analog of diamond.

Our observation that olefinic carbon species exist on the diamond surfaces may seem surprising. However, olefinic carbon species have been shown to exist in bulk type-I diamonds by optical-absorption studies.[53,54] The vibrational lines observed in the bulk diamond at 3107 and 1405 cm^{-1} due to the CH stretch and deformation modes, respectively,[53,54] of the olefinic $=CH_2$ group, are close in energy to the 3070- and 1330–1450-cm^{-1} bands found in the present HREEL spectra, thus rendering support to our interpretation. The presence of olefinic carbon species in bulk diamond were attributed to hydrogen binding to the internal surfaces, such as the surfaces of microscopic voids or to inclusion/diamond interfaces.[54] Microvoids or vacancy complexes are expected to exist on diamond surfaces as a result of polishing, which inevitably gives rise to inherently defective surfaces after preparation. Hydrogenated diamondlike carbon films also have many properties in common with or similar to diamond, because of their similar carbon-bonding characteristics. In particular, both of them are expected to have plentiful defects such as voids. Optical-absorption studies[55] show that a combination of sp^3, sp^2, and sp^1 hybridized carbon atoms simultaneously exist in hydrogenated diamondlike carbon films. Our observation that olefinic CH species exist on the diamond surfaces is thus supported by evidence that such species also exist in hydrogenated diamondlike films.

Despite the good agreement between the present and previous HREEL data[6] about the presence of multiple $CH_{x=1-3}$ species on diamond surfaces and the correlated behavior for silicon surfaces, the nature of CH_x species present on the hydrogen-terminated diamond (111)-(1×1) surface deduced from the HREEL studies is, however, at variance with that from several other measurements. Helium scattering and diffraction data[56] as well as the angular distribution of protons by electron stimulation from H-diamond (111)-(1×1) surfaces[7] suggested that the surface carbon atoms were terminated with a single hydrogen adatom, i.e., H on top sites. Recently, vibrational spectra of the H-diamond (111)-(1×1) surface obtained by using infrared-visible sum-frequency generation[57] showed a single sharp peak at $\sim$2830 cm^{-1}, which was identified as the CH stretch from atomic hydrogen adsorbed on top sites. Despite the support for simple hydrogen truncation of the bulk by proton desorption[7] and helium atom scattering,[56] this model of single H on the top sites simply cannot account for the energy-loss structures between 650 and 1690 cm^{-1} in the HREEL spectra (Fig. 3). The discrepancy among these investigations was noted earlier but no explanation was given.[56,57] Several possible contributing factors to the discrepancy may be hypothesized. For example, the measurement techniques may have different sensitivity depending on the nature of the CH_x species or vibrations. In addition, the diamond samples or surfaces used in the studies may have been different. It is apparent that hydrogen adsorption on diamond surfaces is a complex reaction and that more work is necessary to understand the adsorption process.

The low-energy band in the loss spectrum of the as-loaded diamond surface [Fig. 2(a)] is distinctly different from that in the spectrum obtained from the hydrogen-dosed diamond-H surface previously heated to 1273–1473 K (Fig. 3). However, after heating to 923 K, the energy-loss spectrum of the as-loaded diamond (100) [Fig. 2(c)] became very similar to that of the hydrogen-dosed diamond (100)-H surface [Fig. 3(a)]. It should be pointed out that heating the diamond to 923 K did not change the LEED pattern, showing that reconstruction from (1×1) to (2×1) had not occurred. We interpreted this to mean that as-loaded diamond surfaces are covered with hydrocarbon impurity species. These species were loosely bonded to the surface, and thus were readily desorbed and/or they were converted to $—CH_{x=1-3}$ species on heating to a temperature considerably lower than the temperature at which hydrogen begins to desorb

from the $—CH_{x=1-3}$ species. On storing in an unpumped, high vacuum for extended intervals, the energy-loss spectrum of the diamond (100)-H surfaces [Fig. 2(b)] resembled that of the as-loaded diamond (100) surface [Fig. 2(a)]. This observation implies that hydrocarbon readily adsorbs on diamond surfaces, and that the nature of hydrocarbon contamination on clean diamond surfaces in vacuum is similar to that on the as-loaded diamond surfaces.

It is informative to compare the present chemisorption results with the previous studies of hydrogen desorption from both diamond (111) and (100) surfaces.[7,8] Hamza, Kubiak, and Stulen reported that hydrogen could be driven off to an undetectable level from the diamond (111) surface,[7] but not from the (100) surface.[8] We observed the opposite behavior for hydrogen removal from these diamond surfaces. We note that the desorption measurements of Hamza and co-workers[7,8] monitored hydrogen removed from the surface, while our HREEL experiments measure hydrogen remaining on the surface. Because of the difference in measurement methods, several factors may contribute to the apparent discrepancy. It is widely recognized that hydrogen is a major impurity in diamond.[51] The diamond samples used by Hamza and co-workers and in the present study may contain different hydrogen impurity content in the bulk, which together with hydrogen diffusion to the surface during annealing may give rise to a varying amount of surface hydrogen. Desorption measurement may be sensitive to extraneous hydrogen desorbing from nonsample surfaces, while HREELS only probes the surface-adsorbed hydrogen on the sample. Thus, it is important to ensure that during heating, hydrogen can only emanate from the diamond surface in the desorption measurement. Hydrogen removal from the diamond surface is necessary for continued diamond growth during the CVD process. The relative ease of hydrogen removal from the diamond (100)-H surface in our results may have some relevance to the fact that the best diamond homoepitaxy growth by the CVD process occurs on the (100) diamond surface.[58,59]

V. CONCLUSIONS

The surface phonons on diamond (111)-(2×1) and (100)-(2×1) surfaces, which are almost free and totally free of hydrogen, respectively, have been measured by HREELS. The phonon spectra of the two diamond surfaces are qualitatively similar. At least three phonon loss peaks are positively detected on the diamond (100) surfaces, whereas two phonon loss peaks are positively detected on the diamond (111) surfaces. The measured diamond surface phonon modes agree well with scaled experimental and theoretical phonon modes of the corresponding silicon surfaces. Several modes are detected on diamond surfaces that have not been detected on the corresponding silicon surfaces. The ease of detection of diamond surface phonons and the structural information common to both diamond and silicon should serve to encourage future investigations, both experimental and theoretical.

The features of the energy-loss spectra of the hydrogen-dosed diamond (111)-(1×1)-H and (100)-(1×1)-H surfaces give evidence that the surfaces contain carbon atoms bonded to multiple hydrogens. We propose that coexistence of sp^3 hybridized —CH, $—CH_2$, and $—CH_3$, as well as sp^2 olefinic CH_2, are highly likely on both the (111)-(1×1)-H and (100)-(1×1)-H surfaces. We give evidence that the as-polished, diamond surfaces contain adsorbed hydrocarbon species, that are easily desorbed by heating to 923 K in vacuum. It is found that hydrogen bonded on the diamond (100)-(1×1)-H surface is easily desorbed, while that on the diamond (111)-(1×1)-H surface is more difficult to remove completely.

ACKNOWLEDGMENT

We wish to acknowledge Dr. W. P. McKenna for helpful discussions concerning assignments of CH vibrational modes.

[1]B. B. Pate, Surf. Sci. **165**, 83 (1986), and references therein.
[2]W. A. Yarbrough and R. Messier, Science **247**, 688 (1990), and references therein.
[3]P. G. Lurie and J. M. Wilson, Surf. Sci. **65**, 453 (1977); **65**, 476 (1977).
[4]S. V. Pepper, J. Vac. Sci. Technol. **20**, 213 (1982).
[5]S. V. Pepper, Appl. Phys. Lett. **38**, 344 (1981).
[6]B. J. Waclawski, D. T. Pierce, N. Swanson, and R. J. Celotta, J. Vac. Sci. Technol. **21**, 368 (1882).
[7]A. V. Hamza, G. D. Kubiak, and R. H. Stulen, Surf. Sci. **206**, L833 (1988).
[8]A. V. Hamza, G. D. Kubiak, and R. H. Stulen, Surf. Sci. **237**, 35 (1990).
[9]B. G. Frederick, G. Apai, and T. N. Rhodin, Surf. Sci. **244**, 67 (1991).
[10]W. T. Petrie and J. M. Voks, Surf. Sci. **245**, 315 (1991).
[11]B. G. Frederick, G. Apai, and T. N. Rhodin, Surf. Sci. **275**, 337 (1992).
[12]G. Apai and W. P. McKenna, Langmuir **7**, 2266 (1991).
[13]W. P. McKenna and G. Apai, J. Phys. Chem. **96**, 5902 (1992), and references therein.
[14]B. R. Frieden, in *Deconvolution with Applications in Spectroscopy*, edited by P. A. Jansson (Academic, New York, 1984). The calculations were performed using software by Spectrum Square Associate, Inc. 1988.
[15]S.-Tong Lee (unpublished); the absence of nondiamond carbon was also verified by C 1s Auger line shape.
[16]H. Ibach, Phys. Rev. Lett. **27**, 253 (1971).
[17]N. J. DiNardo, W. A. Thompson, A. J. Schell-Sorokin, and J. E. Demuth, Phys. Rev. B **34**, 3007 (1986).
[18]R. E. Shroder, R. J. Nemanich, and J. T. Glass, Phys. Rev. B **41**, 3738 (1990).
[19]U. Harten, J. P. Toennies, and Ch. Woll, Phys. Rev. Lett. **57**, 2947 (1986).
[20]R. M. Feenstra, W. A. Thompson, and A. P. Fein, Phys. Rev. Lett. **56**, 608 (1986).

[21]A. Stroscio, R. Feenstra, and A. P. Fein, Phys. Rev. Lett. **57**, 2579 (1986).
[22]R. M. Tromp, L. Smit, and J. F. van der Veen, Phys. Rev. Lett. **51**, 1672 (1983); Phys. Rev. B **30**, 2257 (1984); **30**, 6235 (1984).
[23]F. J. Himpsel, P. Heimann, and D. E. Eastman, Phys. Rev. B **24**, 2003 (1981).
[24]R. I. G. Uhrberg, G. V. Hansson, J. M. Nicholls, and S. A. Flodstrom, Phys. Rev. Lett. **48**, 1032 (1982).
[25]D. Straub, L. Ley, and F. J. Himpsel, Phys. Rev. Lett. **54**, 142 (1985).
[26]P. Martensson, A. Cricenti, and G. V. Hansson, Phys. Rev. B **32**, 6959 (1985).
[27]H. Luth, A. Ritz, and R. Matz, Solid State Commun. **46**, 343 (1983).
[28]M. A. Olmstead, Surf. Sci. Rep. **6**, 159 (1987), and references therein.
[29]K. C. Pandey, Phys. Rev. Lett. **47**, 1913 (1981); **49**, 223 (1982); Phys. Rev. B **25**, 4338 (1982).
[30]J. E. Northrup and M. L. Colen, Phys. Rev. Lett. **49**, 1349 (1982); J. Vac. Sci. Technol. **21**, 333 (1882); Phys. Rev. B **27**, 6553 (1983).
[31]T. E. Derry, L. Smit, and J. F. van der Veen, Surf. Sci. **167**, 502 (1986).
[32]G. D. Kubiak and K. W. Kolasinski, Phys. Rev. B **39**, 1381 (1989).
[33]O. L. Alerhand, D. C. Allan, and E. J. Mele, Phys. Rev. Lett. **55**, 2700 (1985).
[34]O. L. Alerhand and E. J. Mele, Phys. Rev. Lett. **59**, 657 (1987); Phys. Rev. B **37**, 2536 (1988).
[35]L. Miglio, P. Santini, P. Ruggerone, and G. Benedek, Phys. Rev. Lett. **62**, 3070 (1989).
[36]L. Miglio, P. Ruggerone, and G. Benedek, J. Electron Spectrosc. Relat. Phenom. **44**, 281 (1987).
[37]W. Goldammer and W. Ludwig, Phys. Lett. A **133**, 85 (1988).
[38]W. Goldammer, W. Ludwig, W. Zierau, and C. Falter, Surf. Sci. **141**, 139 (1984).
[39]J. A. Schaefer, F. Stucki, J. A. Anderson, G. J. Lapeyre, and W. Gopel, Surf. Sci. **140**, 207 (1984).
[40]F. Stucki, J. A. Schaefer, J. R. Anderson, G. J. Lapeyre, and W. Gopel, Solid State Commun. **47**, 795 (1983).
[41]D. J. Chadi, Phys. Rev. Lett. **43**, 43 (1979).
[42]E. J. Mele, D. C. Allan, O. L. Alerhand, and D. P. DiVincenzo, J. Vac. Sci. Technol. B **3**, 1068 (1985).
[43]O. L. Alerhand and E. J. Mele, Phys. Rev. B **35**, 5533 (1987).
[44]D. C. Allan and E. J. Mele, Phys. Rev. Lett. **53**, 826 (1984); Phys. Rev. B **31**, 5565 (1983).
[45]A. Mazur and J. Pollmann, Phys. Rev. Lett. **57**, 1811 (1986).
[46]R. Wehner, H. Borik, W. Kress, A. R. Goodwin, and S. D. Smith, Solid State Commun. **5**, 307 (1967).
[47]G. Herzberg, *Infrared and Raman Spectra of Polyatomic Molecules* (Van Nostrand, Princeton, NJ, 1945).
[48]N. B. Colthup, L. H. Daly, and S. E. Wiberley, *Introduction to Infrared and Raman Spectroscopy* (Academic, New York, 1990).
[49]H. Ibach, H. Hopster, and B. Sexton, Appl. Surf. Sci. **1**, 1 (1977).
[50]L. Pauling, *The Nature of Chemical Bonds,* 3rd ed. (Cornell University Press, Ithaca, NY, 1960), p. 85.
[51]H. Froitzheim, H. Lammering, and H.-L. Gunter, Phys. Rev. B **27**, 2278 (1983).
[52]H. Wagner, R. But, U. Backes, and D. Bruchmann, Solid State Commun. **38**, 1155 (1981).
[53]G. Davis, A. T. Collins, and P. Spear, Solid State Commun. **49**, 433 (1984).
[54]G. S. Woods and A. T. Collins, J. Phys. Chem. Solids **44**, 471 (1983).
[55]B. Dischler, A. Bubenzer, and P. Koidl, Solid State Commun. **48**, 105 (1983).
[56]G. Vidali and D. R. Frankl, Phys. Rev. B **27**, 2480 (1983); G. Vidali, M. W. Cole, W. H. Weinberg, and W. A. Steele, Phys. Rev. Lett. **51**, 118 (1983).
[57]R. P. Chin, J. Y. Huang, Y. R. Shen, T. J. Chuang, H. Seki, and M. Buck, Phys. Rev. B **45**, 1522 (1992), and references therein.
[58]B. V. Derjaguin, B. V. Spitsyn, A. E. Gorodetsky, A. P. Zakharov, L. L. Bouilov, and A. E. Aleksenko, J. Cryst. Growth **31**, 44 (1975).
[59]M. Kamo, H. Yurimoto, and Y. Sato, Appl. Surf. Sci. **33**, 553 (1988).